SCIENTIFIC CULTURE
www.sci-cult.com

SCIENTIFIC CULTURE, Vol. 12, No. 5.1, (2026), pp. 1165-1172
Open Access. Online & Print

DOI: 10.5281/zenodo.12511092

A STUDY OF AERODYNAMICS OF AIRFLOW THROUGH A UAV PROPELLER

Nattaned Kongtabtim[1], Sahatsawat Sangkaeo[2], Pasakorn Kaewphairat[3], Teerawat Klabklay[4]*

[1,2,3] Department of Power Engineering Technology, College of Industrial Technology, King Mongkut's University of Technology North Bangkok, Bangkok, Thailand.
[4] Research Centre for Combustion Technology and Alternative Energy—CTAE and College of Industrial Technology, King Mongkut's University of Technology North Bangkok, Bangkok, Thailand.

Received: 01/12/2025
Accepted: 02/01/2026

Corresponding author: Teerawat Klabklay
(teerawat.k@cit.kmutnb.ac.th)

ABSTRACT

Unmanned Aerial Vehicles (UAVs) or drones are now popular machines used in many fields, including agriculture, surveying, and military missions. Propellers are crucial equipment that generates aerodynamic forces used for propulsion and maneuverability. Although these propellers are commercially available, manufacturers often lack key performance data like thrust and torque at different RPMs, making it hard to choose the best one for a mission. The objective of this study is to simulate the airflow through a UAV propeller using reverse engineering to estimate thrust, torque, mechanical power, and efficiency. The simulation techniques of this study consist of Computational Fluid Dynamics (CFD) and Blade Element Momentum (BEM) theory. Experiments were conducted using a propeller test stand to verify the simulation results. Compared to experimental data between 200 and 4000 RPM, the CFD model demonstrated more accuracy over the BEM. Average CFD errors for thrust, torque, mechanical power, and efficiency were 14.6%, 4.6%, 3.7%, and 11.5% while BEM errors were higher at 25.8%, 13.9%, 18.9%, and 8.6%. The CFD model was more accurate than BEM because it included 3D effects, whereas BEM model relied on simplified 1D analysis.

KEYWORDS: UAV propeller, Computational Fluid Dynamics (CFD), Blade Element Momentum theory (BEM)

1. INTRODUCTION

In the past decade, Unmanned Aerial Vehicle (UAV) technology, commonly known as drones, has undergone rapid development and growth. Originally utilized for military missions, drones now play a significant role in a wide range of industries, including geographical surveying, infrastructure inspection, precision agriculture, as well as transportation and logistics [1]. Moreover, drones enhance accessibility to challenging terrain and improve operational agility, proving to be both effective and cost-efficient tools. Propellers are critical components that significantly impact a drone's flight efficiency and endurance. Although propellers are readily available for purchase from various retailers and online stores in a wide range of shapes, structures, and materials, it has been observed that most commercially available options lack essential specification data, such as thrust and torque at various revolutions per minute (rpm). Such data is crucial for selecting the appropriate propeller for a specific mission [2]. Choosing a propeller that is well-suited to the mission profile is a critical factor influencing the drone's overall performance. A proper propeller design and selection can extend flight duration, decrease energy consumption, and enhance the precision of directional and attitude control. Moreover, it lessens the strain on the motor, resulting in a more durable propulsion system capable of carrying a heavier payload [3]. This study aims to estimate the thrust and torque of a UAV propeller (using a Hobbywing 36190 model as a specific example, as shown in Fig. 1) through reverse engineering and simulation methods.

The research also assesses the accuracy of different simulation models, namely Computational Fluid Dynamics (CFD) and Blade Element Momentum (BEM) theory. Furthermore, experimental measurements were conducted using a propeller test stand to validate the simulation results. A key benefit of this study is that it offers a practical method for estimating propeller performance (thrust and torque) to facilitate the selection of propellers appropriate for a given mission.

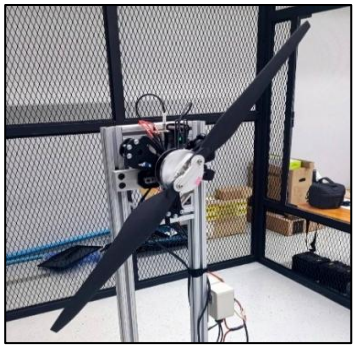

Figure 1: The Hobbywing 36190 propeller

2. METHODOLOGY

2.1. Experimental method

The series 1780 propeller test stand as illustrated in Fig. 2(a) was utilized for the experiments. All necessary devices were installed to measure thrust and torque including rotational speed for a single-motor type. For this study, a Hobbywing 36190 model was used as a rotor specific example for testing. The RCbenchmark software was employed to control the operation and record measurement data [4], as shown in Fig. 2(b).

(a) (b)

Figure 2: 1780 propeller test stand (a) and RCbenchmark software (b)

The Hobbywing 36190 propeller was mounted on a test stand in two configurations as follows: upwind and downwind. These orientations refer to installing the rotor upstream and downstream of the test stand column [5], respectively, as illustrated in Fig. 3. The objective of this experimental setup was to examine the differences in the results arising from these two distinct mounting configurations. The tests were conducted across a rotational speed range of 400 to 2000 rpm.

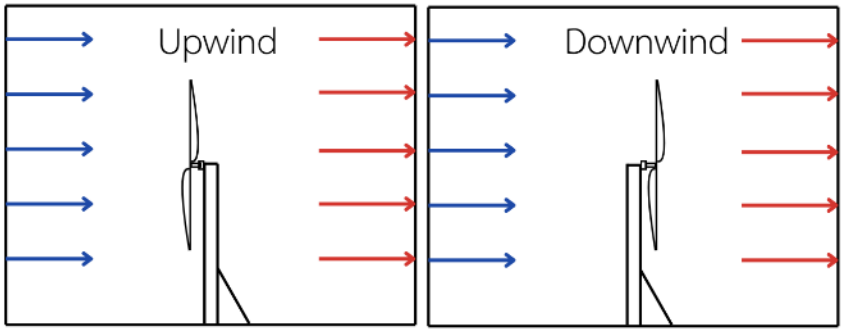

Figure 3: Upwind and Downwind rotor

(a) Mechanical power

Mechanical power (P_{mech}) referred to as shaft power of the propeller, which can be calculated by Eqs. (1).

$$P_{mech} = Q \cdot \omega \qquad (1)$$

where,

P_{mech} is mechanical power (W)
Q is torque driving the propeller (N·m)
ω is angular velocity of the propeller (rad/s)

(b) Propeller efficiency

In this study, propeller efficiency is defined as the ratio between thrust and mechanical power, as expressed in Eqs. (2).

$$\eta = \frac{T}{P_{mech}} \qquad (2)$$

where,

η is propeller efficiency (N/W)
T is thrust generated by the propeller (N)

2.2. CFD simulation

Computational Fluid Dynamics (CFD) is a method used to solve fluid flow problems using numerical analysis, typically based on the finite volume method. It primarily calculates the various forces generated by flow passing through an object. Governing equations consist of the continuity and the Navier–Stokes equation. This study used Reynolds Average Navier-Stokes (RANS) method to analysis the turbulence flow. Therefore, the two governing equations are modified by Reynolds decomposition, as expressed in Eqs. (3) and (4) [6], respectively.

$$\frac{\partial u_i}{\partial x_i} = 0 \qquad (3)$$

$$\frac{\partial}{\partial x_j}\rho\overline{u_\iota}\,\overline{u_j} = -\frac{\partial \bar{P}}{\partial x_i} + \frac{\partial}{\partial x_j}\left(\mu\frac{\partial \overline{u_\iota}}{\partial x_j} - \rho\overline{u_\iota' u_j'}\right) + \overline{F_\iota} \qquad (4)$$

The CFD process with reverse engineering can be separated into three main steps: (i) 3D scanning and CAD modeling, (ii) pre-processing, and (iii) computation and post-processing.

(a) 3D scanning and CAD modeling

The 1.0-m diameter Hobbywing 36190 propeller was 3D scanned as shown in Fig. 4. A corresponding CAD model can then be reverse engineered from the resulting scan data using computer-aided design software [7], as illustrated in Fig. 5.

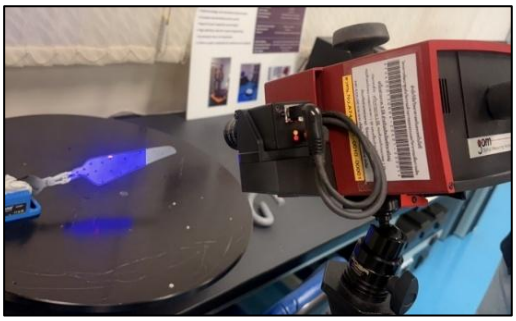

Figure 4: The 3D Scanner

Figure 5: Hobbywing 36190 model created by CAD

(b) Pre-processing

A fluid domain was established to accurately analyze the airflow and forces generated by the rotating Hobbywing 36190 propeller. The domain was created using CAD software and discretized into two regions: a static and a rotating domain. The domain boundaries were categorized into four surfaces: inlet, outlet, symmetry, and wall [8], as typically defined in Fig. 6(a). Mesh generation for the CFD simulation was performed using ANSYS Fluent software, employing a polyhedral mesh with an inflation layer (first layer thickness of 0.00001 meters). The total number of elements was approximately 6,310,000 as presented in Fig. 6(b). The boundary conditions for this study are shown in table I.

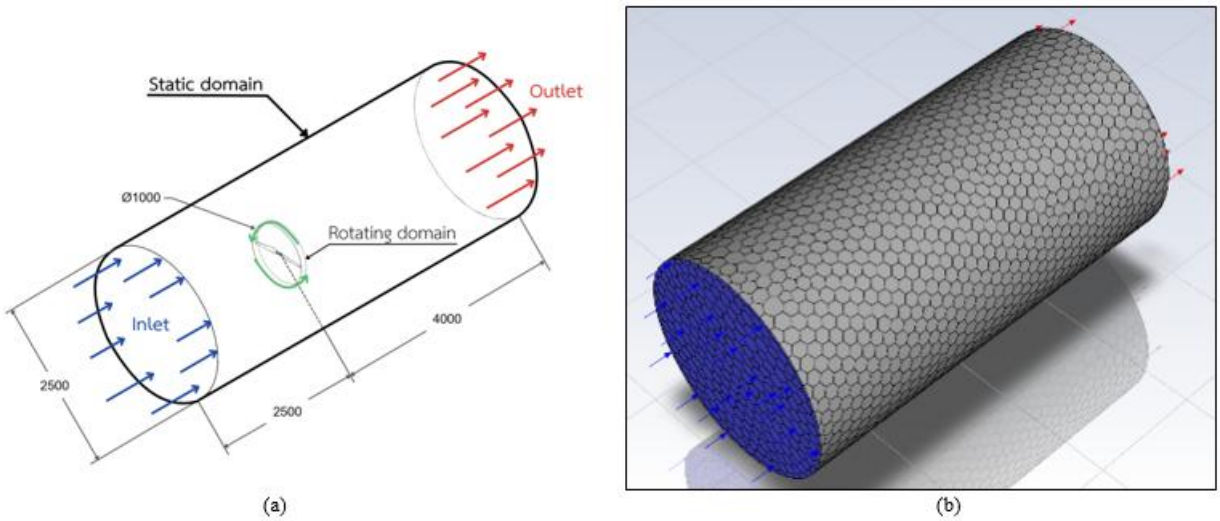

Figure 6: Dimensions of the static and rotating domains (a) and Domain meshing (b)

Table 1: Material properties, boundary conditions, operation, and turbulent model

Parameter	Value	Unit
Air density	1.225	kg/m^3
Air viscosity	1.7894x10^{-5}	kg.m/s
Velocity inlet	0	m/s
Pressure outlet (gauge)	0	Pa
Rotational speed	400-2000	rpm
Turbulent model	$k-\omega$ *SST*	-

(c) Computation and post-processing

Following the configuration of all parameters via the software interface, computations were performed by the system until convergence of all independent variables, including propeller thrust and torque. The CFD simulation results and accompanying graphics are presented in the results and discussion section.

2.3. BEM simulation

Blade Element Momentum (BEM) theory is a method that uses algebraic computations for a system of equations. It is widely applied to estimate the thrust and torque produced by wind turbines or propellers. BEM is composed of two sub-theories: Momentum Theory (MT) and Blade Element Theory (BET). MT estimates thrust and torque through a one-dimensional analysis of the linear and angular momentum of the airflow passing through an annular actuator disc as illustrated in Fig. 7. The velocities at point U_2 and U_4 are modified by the axial induction factor (a).

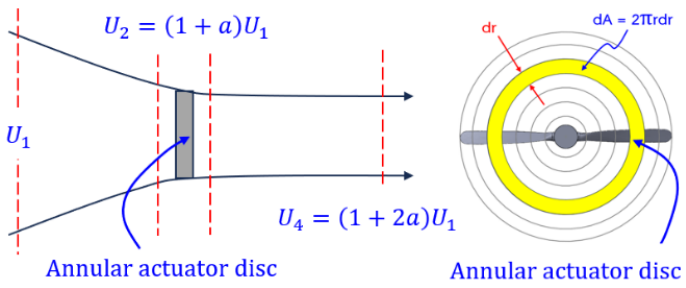

Figure 7: Airflow passing through an annular actuator disc

The momentum equations for elemental thrust (dT) and torque (dQ) are expressed in Eqs. (5) and (6), respectively. The total of the thrust and torque of a blade are subsequently obtained by integrating these elemental contributions.

$$dT = 4a(1-a)U_1^2\rho\pi r dr \quad (5)$$

$$dQ = 4a'(1-a)U_1\rho\pi r^3 dr \quad (6)$$

BET est.s the thrust (dT) and torque (dQ) for each blade section by integrating the aerodynamic forces, which are derived from the angle of attack and blade's cross-sectional shape, as illustrated in Fig. 8.

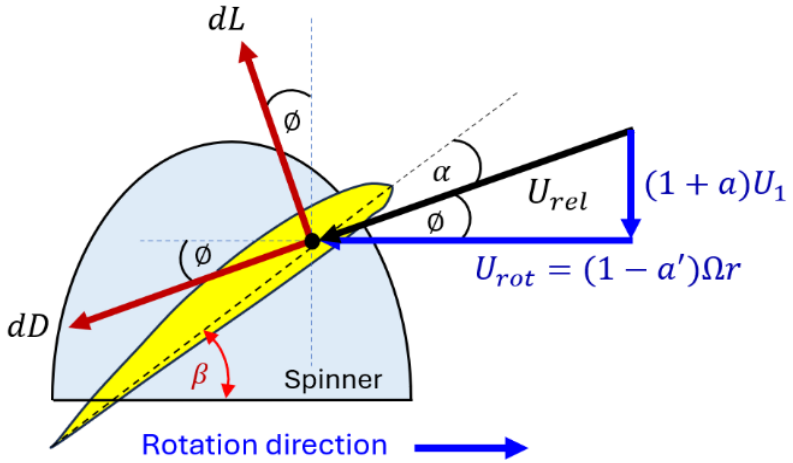

Figure 8: Blade geometry for analysis of propeller

The blade element equations for elemental thrust and torque are presented by Eqs. (7) and (8), respectively. The total thrust and torque for the entire rotor can then be obtained by integrating these elemental contributions across the blade span and multiplying by the number of blades (B).

$$dT = \frac{1}{2}\rho c dr U_{rel}^2 \cdot C_n \cdot B \quad (7)$$

$$dQ = \frac{1}{2}\rho c dr U_{rel}^2 \cdot C_t \cdot r_{avg} \cdot B \quad (8)$$

The angle of relative velocity and the angle of attack are defined by Eqs. (9) and (10), respectively.

$$tan\phi = \frac{(1+a)U_1}{(1-a')\Omega r} \quad (9)$$

$$AOA = \beta - \phi \quad (10)$$

By eliminating dT and dQ and combining the MT and BET [9], the BEM equations are rearranged into Eqs. (11) and (12).

$$a = \frac{1}{\frac{4sin^2\phi}{C_n\sigma'} - 1} \quad (11)$$

$$a' = \frac{1}{\frac{4sin\phi cos\phi}{C_t\sigma'} + 1} \quad (12)$$

where,

$$C_n = C_l cos\emptyset - C_d sin\emptyset \quad (13)$$

$$C_t = C_l sin\emptyset + C_d cos\emptyset \quad (14)$$

The blade data of the Hobbywing 36190, which is required in BEM simulation, can be presented in two sections: cord and pitch angle, as shown in Table II.

Table 2: Blade data of hobbywing 36190

Radius (m)	Chord (m)	Pitch (degree)
0.10	0.0543	13.8
0.14	0.0671	16.1
0.20	0.0559	13.5
0.25	0.0478	12.1
0.35	0.0363	9.7
0.46	0.0177	1.5

The lift and drag coefficients of the Hobbywing 36190 propeller were estimated at xx positions of blade span using a 2D-RANS CFD for an angle of attack range of -20 to 20 degrees [10]. These results were then extended to a full range of -90 to 90 degrees by using the Viterna and Corrigan post-stall model [11], as presented in Fig. 9. For the final step, a sequential simulation technique can be applied to solve the system of BEM equations iteratively, as illustrated by the diagram in Fig. 10. The BEM results are exhibited in the results and discussion section.

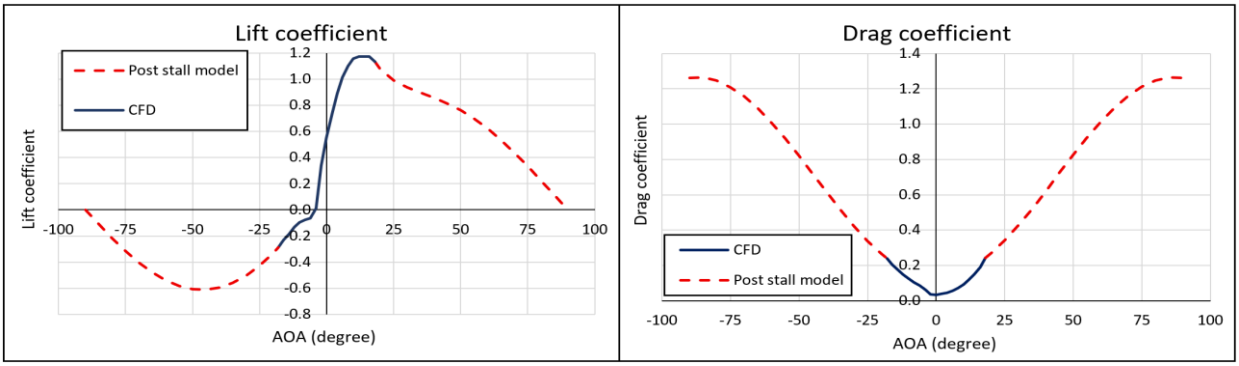

Figure 9: C_l and C_d from 2D-RANS CFD and Post-stall model at the radius 0.10 meters

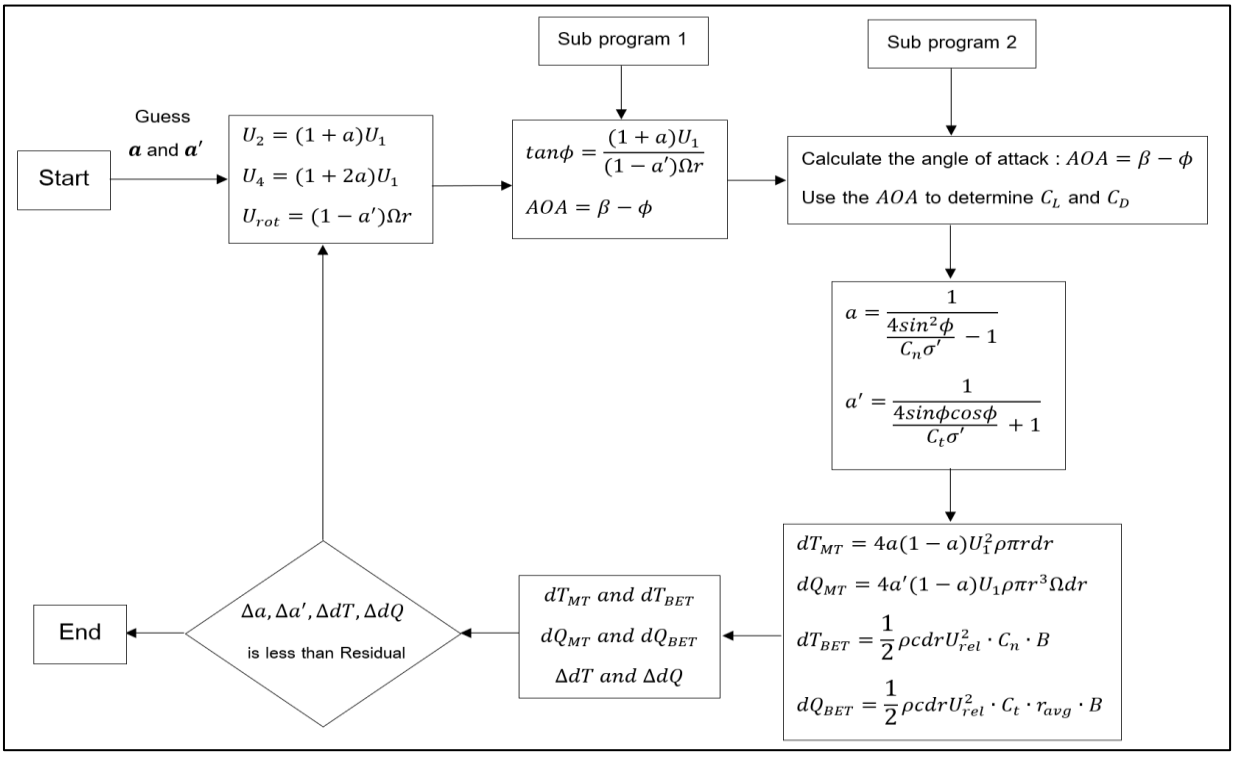

Figure 10: Flowchart: step-by-step procedure for BEM computation.

3. RESULT AND DISCUSSION

3.1. Experimental results

According to Hobbywing 36190 testing conducted by the series 1780 propeller test stand, the experiment revealed only a bit difference between upwind and downwind rotor configurations. The results indicated that both the thrust and torque produced by the two configurations were very similar. The average error for the thrust was approximately 3.8%, while for the torque it was around 7.2%, as illustrated in Fig. 11.

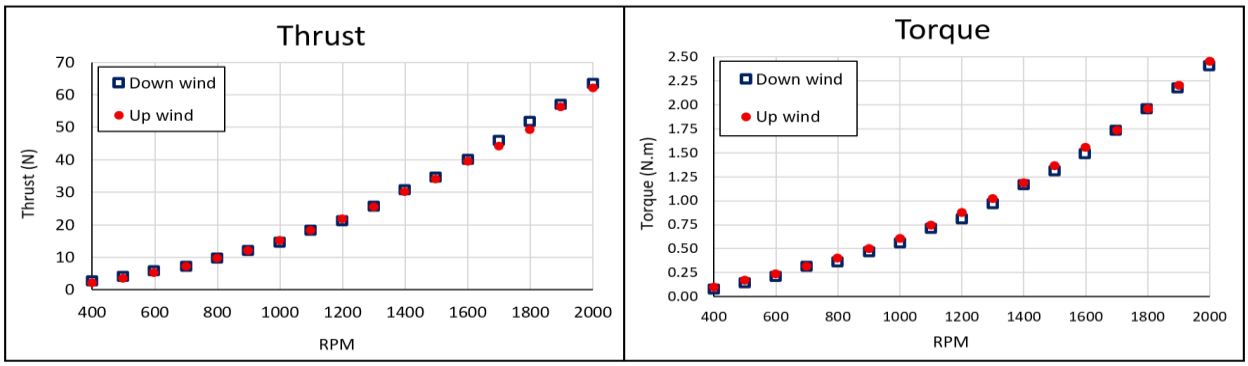

Figure 11: The thrust and torque of Hobbywing 36190 propeller obtained by the series 1780 propeller test stand

3.2. CFD and BEM simulation results

According to the CFD analysis, as illustrated by the graphic results in Fig. 12(a), the thrust of the propeller was generated by the pressure differences around the propeller at any RPMs. The velocity contour can be shown in Fig. 12(b).

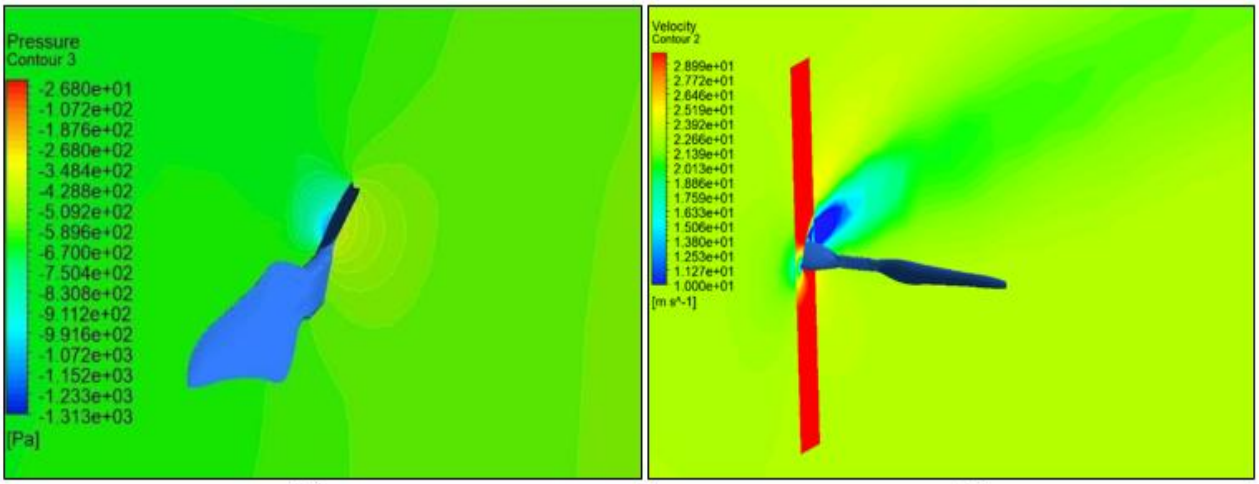

Figure 12: The result of Pressure contour (a) and The result of Velocity contour (b) at 1,000 rpm

The results of thrust and torque from CFD model were significantly more accurate than BEM theory model. For the thrust estimation, The CFD's average error was approximately 14.6%, while BEM provided a higher error of roughly 25.8%, as shown in Fig. 13(a). For the torque estimation, the CFD's average error was much lower at about 4.6%, compared to the BEM's approximately 13.9%, as presented in Fig. 13(b).

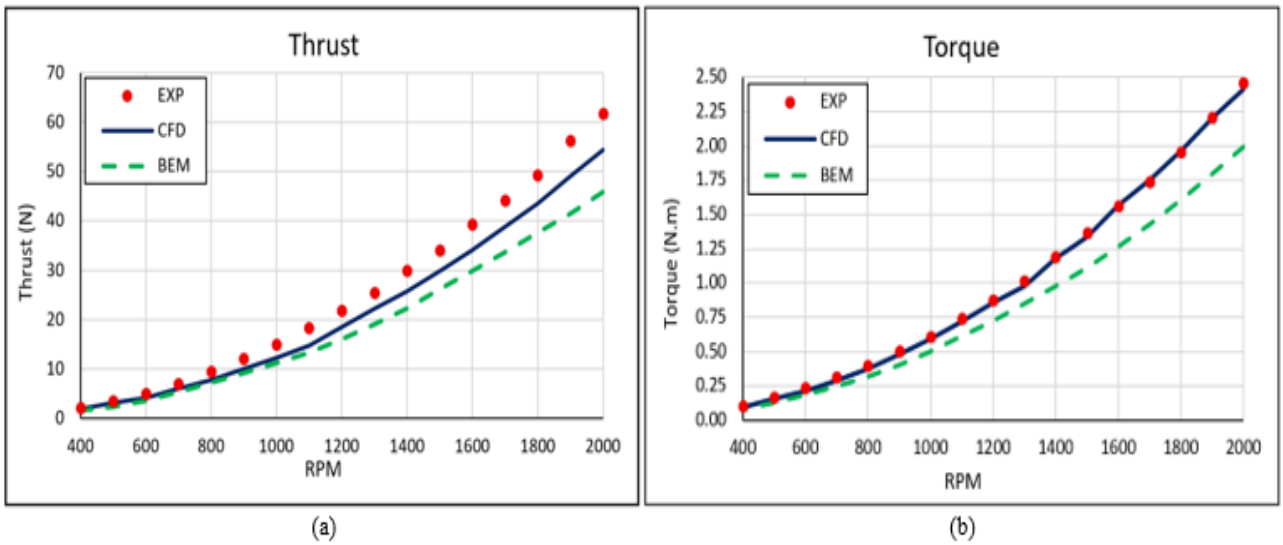

Figure 13: Comparison of thrust (a) and torque (b): experiment, CFD, and BEM simulation.

It was observed that the BEM estimation exhibited significantly larger underestimation errors compared to the CFD results. This discrepancy was attributed to the lift and drag coefficients applied in Eqs. (13) and (14), which were merely derived from a simplified 2D CFD estimation. This 2D approach proved insufficient for capturing 3D rotational effects, specifically the centrifugal and Coriolis forces present under actual operating conditions. Additionally, the lift and drag coefficients for high angles of attack were appraised using Prandtl's post-stall model, as shown in Fig. 9. Furthermore, the errors from both CFD and BEM progressively increased with higher rpm due to a cumulative effect. The mechanical power derived from experimental, CFD, and BEM results as shown in Fig. 14(a) exhibited a similar trend compared to the torque lines in Fig. 13(b) but appeared slightly more curvilinear. This is because the mechanical power is a function of both torque and rotational speed, as shown in Eq. (1). The average errors in mechanical power of CFD and BEM were about 3.7% and 18.9%, respectively. The errors in mechanical power were likely due to the torque estimation.

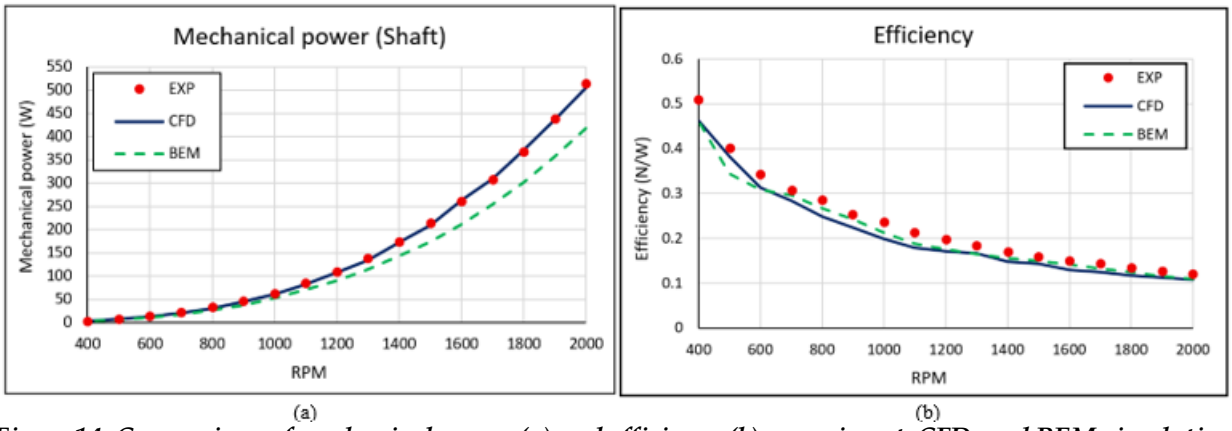

Figure 14: Comparison of mechanical power (a) and efficiency (b): experiment, CFD, and BEM simulation.

Propeller efficiency results from both CFD and BEM simulations correlated very well with the experimental measurements throughout the RPM range. It was observed that operation at lower RPMs is likely to result in higher efficiency.

4. CONCLUSIONS

The objective of this study is to simulate the airflow through a UAV propeller to estimate thrust, torque, mechanical power, and efficiency by the two techniques consisting of CFD and BEM models. The results showed that the CFD demonstrated more accuracy over the BEM. Average CFD errors for thrust, torque, mechanical power, and efficiency were 14.6%, 4.6%, 3.7%, and 11.5% while BEM errors were higher at 25.8%, 13.9%, 18.9%, and 8.6%. The CFD model was more accurate than BEM because it included 3D effects, whereas BEM model relied on simplified 1D analysis.

ACKNOWLEDGEMENT

This research was supported by Techno Park, King Mongkut's University of Technology North Bangkok.

REFERENCES

[1] J. Natthawut, M. Phitnari, C. Chairat, et. al., Attitudes and awareness regarding safety of using unmanned agricultural aircraft, Administrative journal for local development, 2025, 4(1), 57–70.

[2] J. Wanchai, B. Oran, and T. Kamon, Experimental investigation on motor and propeller efficiency of tailless mini UAV, *NKRAFA journal of science and technology*., 2020, 16(2), 1 – 12.

[3] Y. Patel, A. Gaurav, K. Srinivas, et. al.,A Review on Design and Analysis of the propeller used in UAV, International Journal of Advanced Production and Industrial Engineering, IJAPIE-SI-IDCM 605, 2017, 20–23

[4] M. Wojtas, P Wyszkowski, M. Madro, et. al., Test stand for propellers and rotors in VTOL drone systems, Transactions on Aerospace Research eISSN 2545-2835 ,VOL. 270, NO. 1/2023, 67-85

[5] A. B. Weishaupl, S. D. Prior, Influence of Propeller Overlap on Large Scale Tandem UAV Performance, Unmanned Systems, Vol. 04, No. 07, 2019, 245-260

[6] W. Piluck, K. Sangnak, A. Arbubaka, et. Al., The Effect of Pitch Angle Amplitudes on a Cyclorotor Performance Using Computational Fluid Dynamics, International Journal of Mechanical Engineering and Robotics Research, Vol. 14, No. 5, 2025

[7] E. B. Njaastad, S. Steen, O. Egeland, Identification of the geometric design parameters of propeller blades from 3D scanning, Journal of Marine Science and Technology, 2022, Vol. 27, 887–906

[8] M. Rajendran, M. Arumugam, L. Sourirajan, et. al., Multi-dimensional analysis of the hybrid profiled propeller of a pentacopter UAV: Aerodynamic, aero-acoustic, and structural parametric estimations utilizing synergistic engineering approaches, Results in Engineering 26, 2025

[9] T. Klabklay, W. Sridech, Blade element momentum theory for estimating efficiency of Thai sail windmill, The Journal of Industrial Technology, 2019, 15(3), 93-103.

[10] J. R. Portela, O. L. Danguillecourt, V. I. Oliva, et. al., The Effect of Airfoil Geometry Variation on the Efficiency of a Small Wind Turbine, Technologies, 2025, 104614

[11] J. Tangler, J. D. Kocurek, Wind Turbine Post-Stall Airfoil Performance Characteristics Guidelines for Blade-Element Momentum Methods, National Renewable Energy Laboratory, 2004